Acta Geotechnica (2007) 2:1–15
DOI 10.1007/s11440-007-0027-y

REVIEW ARTICLE

Compaction localization in the Earth and the laboratory: state of the research and research directions

David Holcomb · John W. Rudnicki · Kathleen A. Issen · Kurt Sternlof

Received: 16 October 2006 / Accepted: 21 March 2007 / Published online: 14 April 2007

Abstract Localized compaction in porous rocks is a recently recognized phenomenon that has been shown to reduce permeability dramatically. Consequently, the phenomenon is relevant to a variety of technologies involving fluid injection or withdrawal. This article summarizes current understanding of localized compaction and impediments to further progress. The article is based on discussions at a small workshop on localized compaction sponsored by the Office of Science, U. S. Department of Energy.

Keywords Compaction localization · Bifurcation

D. Holcomb (✉)
Sandia National Laboratories,
Albuquerque, NM 87123-0751, USA
e-mail: djholco@sandia.gov

J. W. Rudnicki
Department of Civil and Env. Engineering,
Northwestern University, 2145 Sheridan Road,
Evanston, IL, USA
e-mail: jwrudn@northwestern.edu

K. A. Issen
Wallace H. Coulter School of Engineering,
Clarkson University, 207 CAMP, Box 5725,
Potsdam, NY 13699-5725, USA
e-mail: issenka@clarkson.edu

K. Sternlof
Harvard Design & Mapping,
125 Cambridgepark Drive,
Cambridge, MA 02140, USA
e-mail: ksternlof@hdm.com

1 Compaction localization: state of knowledge

Over the past decade a new mode of deformation in porous, granular rocks has been recognized and investigated: compaction localization. Compaction localization is a limiting case of shear localization with compaction in which macroscopic shear deformation is absent. In both shear localization and pure compaction localization a material responds to compressive stresses, not by homogeneous deformation, but instead by concentrated deformation in a well-defined zone. The faulting produced by shear localization is central to the solid earth sciences and it is anticipated that localized compaction and the associated permeability reduction will also be of high importance. In particular, current work shows that compaction localization is most likely to occur in clastic sedimentary rocks with porosities in excess of about 16%. These formations are of great economic importance as oil and gas reservoirs [48] and are relevant to a variety of other applications including aquifer management, sequestration of CO_2 [72] and hazardous waste disposal. A phenomenon that acts to reduce permeability and compartmentalize fluid flow has the potential for economic, environmental and social impacts.

In October, 2004 a workshop brought together field geologists, experimentalists, theoreticians and numerical modelers (see Table 1) to examine the state of research in this area, grapple with the discrepancies between experimental results, discuss the relevance of laboratory experiments to field observations, and consider the implications of the phenomenon of compaction localization for geosciences, geotechnology and material science. This summary report discusses the issues and questions that drive research and interest in compaction localization.

Table 1 Compaction workshop participants

Atilla Aydin	Stanford University	aydin@pangea.Stanford.EDU
David Boutt	Sandia National Laboratory (now at University of Massachusetts)	dfboutt@sandia.gov, dboutt@geo.umass.edu
Vennela Challa	Clarkson University	vennelac@gmail.com
Eric Grueschow	Northwestern University (now at ExxonMobil Upstream Research)	eric.r.grueschow@exxonmobil.com
Bezalel Haimson	University of Wisconsin	bhaimson@wisc.edu
David Holcomb	Sandia National Laboratory	djholco@sandia.gov
Rune Holt	SINTEF Petroleumsforskning	Rune.Holt@iku.sintef.no
Kathleen Issen	Clarkson University	issenka@clarkson.edu
Stelios Kyriakides	University of Texas at Austin	skk@mail.utexas.edu
Neal Nagel	ConocoPhillips	Neal.Nagel@conocophillips.com
William Olsson	Sandia National Laboratory	waolsso@sandia.gov
David Pollard	Stanford University	dpollard@pangea.stanford.edu
John Rudnicki	Northwestern University	jwrudn@northwestern.edu
Kurt Sternlof	Stanford University	kurtster@pangea.stanford.edu
Sheryl Tembe	SUNY Stony Brook	stembe@ic.sunysb.edu

1.1 Field evidence related to compaction localization

Deformation bands are tabular zones of concentrated strain in rock that lack discrete surfaces of displacement discontinuity, such as a surface of separation [1, 2, 4]. Bands exhibiting predominantly shear strain have been studied observationally since the late 1970's and are extremely common in clastic rocks. Aydin and Johnson [3] connected the formation of such deformation bands to strain localization theory [8, 55, 60]. The orientation of deformation bands was predicted to be a function of material constitutive properties and stress state [8, 32, 59, 60]. Theory predicts that possible angles between the normal to the deformation band and the maximum compressive stress range from 0° to 90°. In laboratory axisymmetric compression tests, this angle is typically 50° to 60°. In the field the orientation of the maximum compressive stress is seldom known with certainty but the angle between the band normal and the inferred orientation of the maximum compressive stress is often similar to that observed in the laboratory.

In contrast to shear localization, there are only a few well documented examples of naturally occurring compaction localization. Not until 1996 were field examples of deformation bands described as lying normal to the inferred local direction of maximum compression ($\theta = 0°$) named ''compaction bands'' by Mollema and Antonellini [41]. More recently, Du Bernard et al. [13] have described deformation bands interpreted as accommodating pure dilation ($\theta = 90°$). The compaction bands (CBs) described by Mollema and Antonellini [41] in the eolian Jurassic Navajo Sandstone of southeastern Utah are tabular in form, 0.1 to 1.5 cm thick, up to several meters in trace length, and commonly occur within the compressional quadrants of shear-band faults such that they trend normal to the inferred direction of local maximum compression. Little or no measurable shear offset was detected across these bands and, despite considerable grain fracturing, grain crushing and comminution were limited. Nonetheless, micrographic analysis revealed that the bands are structures where significant pore volume reduction had occurred.

Deformation bands identified as dominated by compaction also occur in the Aztec Sandstone—a depositional and stratigraphic equivalent of the Navajo Sandstone that is expansively exposed at the Valley of Fire State Park in southeastern Nevada (Fig. 1). First studied by Hill [27], who noted the general lack of apparent shear offset in outcrop, the descriptions of these structures by Sternlof [63] and Sternlof et al. [64, 66; 67] comprise the most extensive analysis of naturally occurring CBs to date. The bands in the Aztec Sandstone are similar to those described by Mollema and Antonellini [41] in terms of thickness and microstructure, but are generally much longer, tending to be tens of meters long. In addition, they do not appear to be subsidiary structures associated with faults. In fact, their pervasive distribution and general consistency of orientation, coupled with a marked tendency toward curving tip patterns indicative of mechanical interaction, suggest a tectonic-style fabric of localized compaction analogous, but opposite in kinematic sense, to those that have been well documented for opening-mode cracks [63, 67] such as joints, veins and dikes (e.g. [54]).

As exposed in the Valley of Fire, the 1,400-m-thick Aztec Sandstone comprises a type locality for CBs in

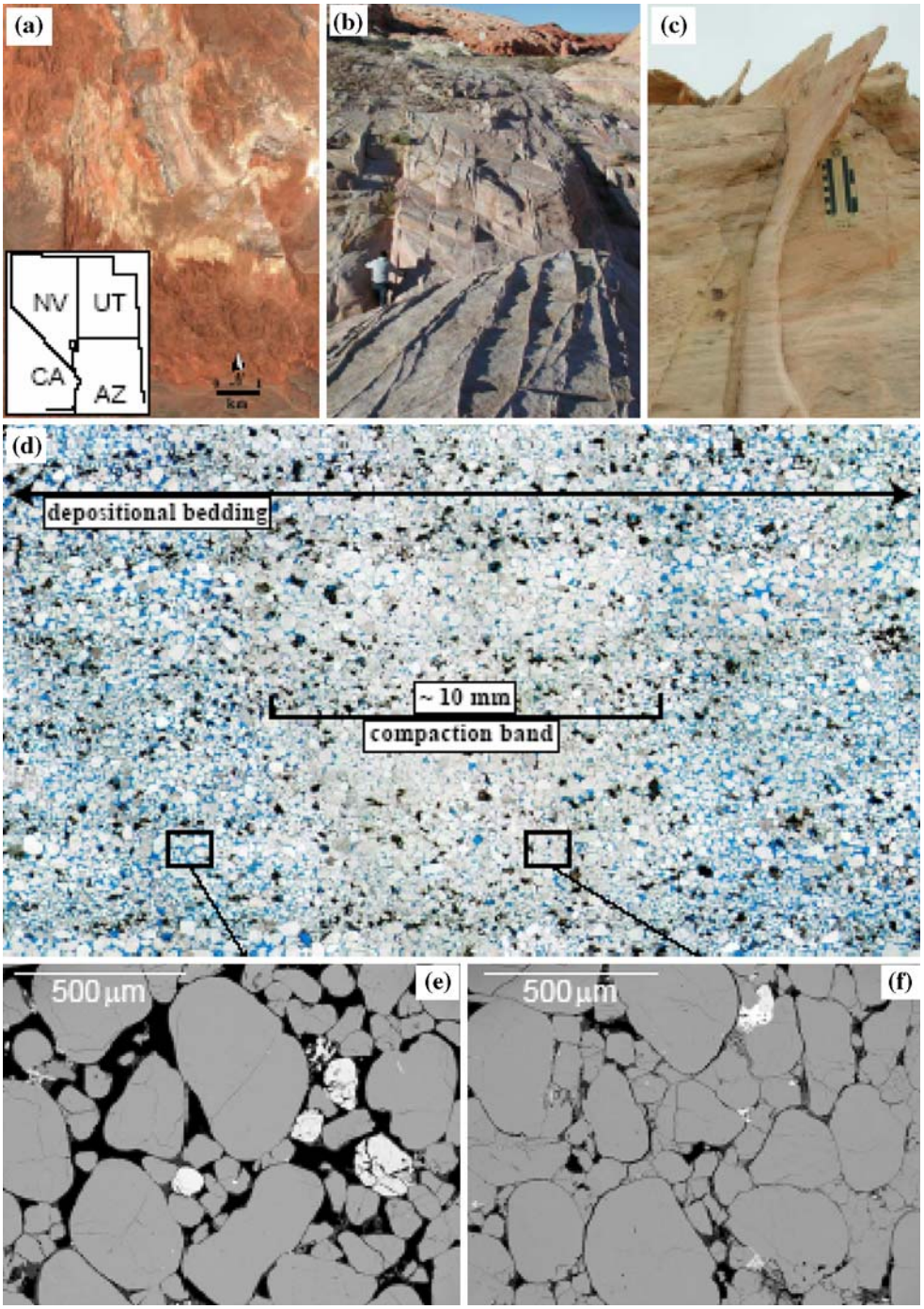

Fig. 1 Images depicting compaction bands in the Aztec Sandstone at the Valley of Fire State Park, southeastern Nevada (adapted from [63]). **a** Air photo of study area showing expansive outcrop exposure (approximate location of air photo indicated on inset diagram). **b** Typical view of subparallel, anastomosing compaction band array (resistant fins) in outcrop. View is to the north-northwest along the dominant band trend. **c** Close-up view of compaction band fin capturing its essential tabular-planar aspect, centimeter thickness and lack of obvious shear displacement. **d** Photomicrograph mosaic of a compaction band at high angle to depositional bedding, which passes through the band with no apparent shear offset, change in direction or change in thickness. This suggests that uniaxial compaction perpendicular to the band predominates. White grains are quartz, dark grains are mostly stained orthoclase and some hematite, blue is epoxy-filled pore space. **e** Backscatter electron image from just outside the compaction band. *Light gray* is quartz, off-white is orthoclase, *dark gray* is kaolinite, *stark white* is hematite, *black* is pore space. **f** Backscatter electron image from inside the compaction band. Note the abrupt drop in porosity, pore size and pore connectivity accommodated by intense damage to some quartz grains. These petrophysical changes account for the permeability and fluid flow impacts of compaction bands, individually and in aggregate

reservoir-quality rock. Here the bands tend to weather out in positive relief as tabular fins at high angle to depositional bedding, revealing systematic outcrop-scale patterns that range from nearly parallel sets of very planar bands, to two nearly orthogonal sets of mutually cross-cutting bands, to more seemingly erratic, anastomosing variations [63, 64]. Microscopy reveals that primary compaction within these CBs is the result of quartz grain deformation accommodated by intense intra-granular fracturing, leading to a sharp drop in porosity from about 25 to 15% accomplished across zones ranging from just a few grain diameters wide (~0.5 mm) to as much as a few cm wide. Subsequent accumulation of clay within the bands further reduced residual porosity to about 10% or less, while rendering them preferentially cemented relative to the surrounding sandstone and thus more resistant to erosion in outcrop. Across planar sections of the bands (i.e. away from mechanical interactions that cause curving) compaction appears to occur with little or no shear, as demonstrated by the absence of offset depositional bedding and/or disaggregation of otherwise heavily fractured grains [63, 67].

Their variety of patterns in outcrop notwithstanding, the gross geometry of individual CBs in the Aztec Sandstone is that of very thin inclusions of uniaxially compacted grains formed within otherwise uniform sandstone. Occasional exposures in areas of appreciable relief (tens of meters) do indicate that individual bands are grossly disc shaped (i.e. relatively oblate). Viewed at the scale of hundreds of meters, an anastomosing pattern of north-trending, steeply east-dipping bands predominates. The dominance of this trend suggests a regional east–west direction of maximum compression during band formation, locally complicated by mechanical heterogeneity related to the complex sedimentary architecture of the eolian sandstone. This interpretation is consistent with the inferred direction of tectonic transport and maximum compression associated with Cretaceous overthrusting of the Sevier orogeny [27, 63, 67].

For reasons not yet entirely understood, CBs are abundant only in the upper half of the Aztec Sandstone, suggesting a lower burial limit on the material and/or loading conditions conducive to compaction failure. Geological evidence for the depositional, burial, tectonic and diagenetic history of the Aztec Sandstone [14] does provide constraints on the material conditions and regional state of stress extant during compaction band formation [67]. The CB-genic zone ranged from sandstone lightly cemented with hematite and/or clay, as it is today, to essentially uncemented granular material, and presumably it was fully saturated and unconfined. It is also probable that CBs formed prior to discontinuous loading by the easternmost Sevier thrust sheets, and thus also before deposition of most of the 1,600 m of post-Jurassic sediments found in the area. Thus, at the time of CB formation, vertical overburden loading ranged anywhere from a few MPa up to about 30 MPa, accompanied by pore pressures of less than 13 MPa. This in turn suggests that the maximum principal tectonic stress associated with CB formation could have ranged up to little more than 60 MPa [67].

In conclusion, field evidence suggests that CBs formed pervasively throughout the upper Aztec Sandstone as discrete structures of highly localized, grain-failure compaction within a weakly cemented, porous granular material subjected to modest burial and tectonic stresses. Furthermore, the net shortening associated with extensive CB formation across the entire Valley of Fire area is on the order of 1% or less [63, 67].

1.2 Experimental investigations

1.2.1 Axisymmetric compression loading

Several laboratory investigations have produced evidence of localized compaction in porous rock, with one or more planar bands oriented roughly perpendicular to the direction of maximum shortening [6, 17, 19, 20, 22, 24, 45, 46, 75]. These investigations have, however, produced three different patterns of bands. Two of these have been observed in axisymmetric compression loading of nominally homogeneous samples. The third has been observed in the heterogeneous stress field created by the presence of a borehole in a block loaded by three different principal stresses.

Olsson [45], Olsson and Holcomb [46] and Holcomb and Olsson [28] observed one pattern of compaction localization in axisymmetric compression tests on an analogue reservoir rock, Castlegate sandstone. One or two bands appear in the specimen and grow in thickness with increasing loading until the entire specimen is covered. The second pattern consists of thin bands that can spread across the specimen sequentially with increasing applied deformation. The bands are interlayered with less deformed material. Individual bands of this type have also been observed to grow in-plane across the width of the specimen from a stress concentration [69, 71]. More thin bands are added sequentially along the length of the specimen as overall strain increases. The third pattern is a single band that forms in a heterogeneous stress field created by the presence of a hole in a stressed block. The band has a constant thickness of 5 to 10 grain diameters and propagates in its own plane.

All three patterns of bands form in porous sandstones that do not exhibit obvious differences that could be correlated with the different patterns. It is not known why experiments appear to produce three apparently different patterns of compaction bands, or whether they are simply

different manifestations of the same phenomenon. But because of the distinct effects that the various types of bands may have on reservoirs or aquifers, it is important to understand their causes.

In initial investigations motivated by the field observations of Mollema and Antonellini [41], Olsson [45] conducted conventional triaxial compression tests at confining pressures up to 100 MPa on an analogue reservoir rock, Castlegate sandstone. He observed high-angle (measured between the normal to the band and specimen axis) shear bands at the lower pressures and compaction bands for confining pressures between 69 and 100 MPa. In later experiments [46], analysis of acoustic emissions (AE) occurring during deformation confirmed that not only do compaction bands form, but, as suggested earlier [45], they grow in thickness during continuing deformation of the specimen. The bands initially appear near the ends of the specimen, presumably due to the deviation from homogeneous stress field caused by the end conditions.

The key phenomenological data for Castlegate sandstone undergoing compaction banding are summarized in Fig. 2 (similar to data shown in Fig. 4 of Olsson and Holcomb [46]) which plots the stress difference $\sigma_D = \sigma_{11} - \sigma_{33}$ as a function of nominal axial strain (Because the sample is deforming nonhomogeneously, nominal strain ε_{11} is defined as the change in length divided by original specimen length). Comparison of the peak in σ_D near $\varepsilon_{11} = 0.01$ with the AE locations confirms that this corresponds to the stress at which the initial band or bands form. The pertinent features of the stress–strain curve shown in Fig. 2 are the nearly linear behavior prior to the stress peak, followed by a small stress drop of about 5 MPa at a strain of 0.01. An approximately flat region follows this drop to a strain of about 0.08, where the stress begins to rise. Acoustic emission locations show that bands appear at both ends of the sample at the first peak in stress. They then grow in thickness while the specimen deforms at nearly constant stress (flat portion of the curve), merging at the up-turn in stress near $\varepsilon_{11} = 0.08$ (Fig. 2).

The subpanels of Fig. 2 illustrate the evolution of the compaction localization by plotting the locations of acoustic emissions, projected on a plane parallel to the sample axis, occurring during the marked portion of the stress versus nominal strain curve. As the applied deformation proceeds, the principal locations of AE move toward the center of the specimen where they merge. Experiments in which the compaction process was not carried to completion allowed examination of the effect of the compaction localization process on the sandstone grains and structure. For portions of the specimen where compaction localization had occurred, as indicated by the passage of the AE front or density peak, post-test examination showed the material was uniformly crushed [12]. Material from the region between the fronts that had not experienced compaction localization was essentially unfractured. Thus these AE fronts define the transition zones or boundaries between the compacted and uncompacted sandstone; Olsson and Holcomb [46] referred to these zones as compaction fronts and a simple kinematic model of Olsson [47] showed that the speed of the fronts was related to rate of imposed strain and the porosity jump across the band.

Wong and co-workers [6, 39, 71, 75] have reported the second pattern of localized compaction, an example of which is shown in Fig. 3. They have observed discrete, thin (~0.1 mm), somewhat wavy compaction bands in Rothbach, Berea, Diemelstadt, and Bentheim sandstones. The associated stress–nominal strain curves have a saw-tooth appearance. The local stress drops appear to correlate with the formation of individual bands and with spikes in the acoustic emission rate. As observed in the experiments on Castlegate sandstone, the bands form first near the ends of the sample. However, in contrast to the widening zones of uniform compaction in the Castlegate, thin (widths of only a few grains), discrete bands of crushed material are interlayered with uncrushed material. This interlayered pattern then spreads towards the center of the specimens with continued deformation. After sufficient axial shortening, the entire specimen appears layered [6].

1.2.2 In-plane propagation initiated by stress concentrators

Haimson and coworkers have observed a third pattern of compaction localization in experiments on pressurized boreholes in pre-loaded rock blocks. Haimson and Song [25, 26] found that in Berea sandstone with a porosity of 17% normal ''V-shaped'' breakouts formed near boreholes drilled in blocks subjected to three different normal (principal) stresses on the faces of the block. In contrast, for Berea sandstone of 22.5% porosity, long slots normal to the maximum applied compression extended from the boreholes. Examination of further experiments at different stages of slot formation indicated that the slots propagated by creating a zone of crushed and disaggregated material ahead of the slot (Fig. 4). Circulating pore fluid then removed this material. Thus, the slot-like breakouts appear to be washed-out compaction bands [19]. Haimson [20] and Haimson and Kovacich [23] observed slots 5–10 grain diameters wide in Berea of 25% porosity and found that the slot lengths could be as much as three times the diameter of the borehole. Testing of samples of St. Peter sandstone with two different porosities indicated differences in the compaction zone in front of the slot. For St. Peter sandstone with porosity in the 11–12% range the material ahead of the slot contained crushed grains; for the higher porosity

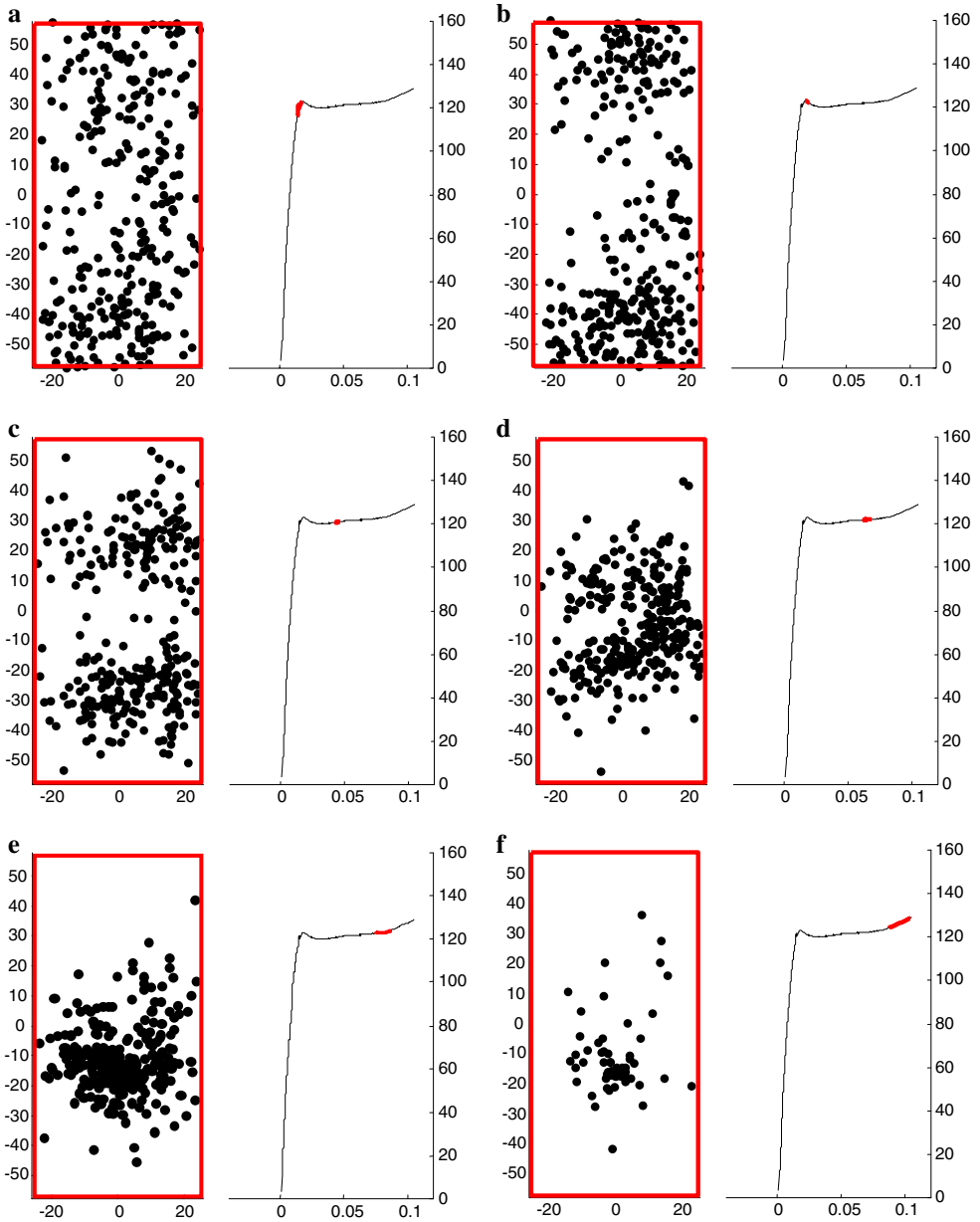

Fig. 2 Characteristic behavior of a porous sandstone (Castlegate) during the formation and propagation of compaction bands. Locations of AE events shown by dots on a schematic cross-section of specimen in left-hand panel in each pair. The right-hand panels show axial stress plotted against nominal strain. The thickened, red segment of the stress-strain curve is the window during which the AE events occurred. **a** pre-peak, pre-localization, events randomly distributed; **b** at peak, localization occurring, events concentrated in bands; **c** localization proceeding at near-constant stress, locus of events moving toward mid-point of sample; **d** event bands beginning to coalesce; **e** compaction nearly completed as event bands coalesce; **f** compaction completed, stress begins to rise

samples, in the 16–22% range, the grains ahead of the slot were intact but compacted, as inferred from the reduced 2-D porosity estimates on electron backscatter images [22, 38].

Relatively high porosity (greater than 10%) appears to be necessary for formation of compaction bands. Yet the failure to observe compaction bands in sandstones having the requisite porosity suggests that other factors are also important. Recent drilling experiments suggest that rock mineralogical composition and presence of cement has a significant influence [24]. One sandstone with a porosity of 28%, Tablerock, exhibits normal V-shaped breakouts and no compaction bands. It is composed of 55% quartz and 37% feldspar, with some quartz cement. Another sandstone, Mansfield, has a similar porosity (26%), but does form compaction bands. It is composed of 90% quartz, and is ''spot-sutured'' with quartz. In fact Haimson and his group have tested six different sandstones varying in

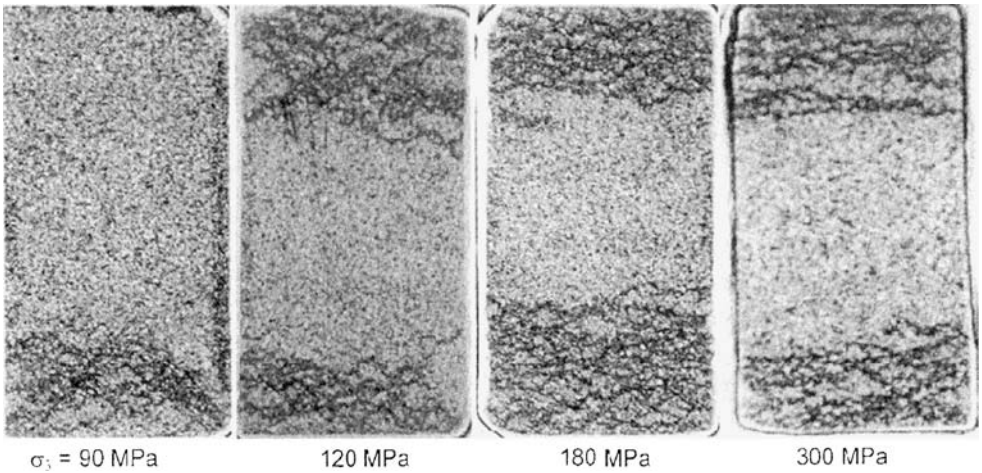

Fig. 3 Discrete, thin (~0.1 mm), somewhat wavy compaction bands formed at several pressures in sandstone (adapted from [75])

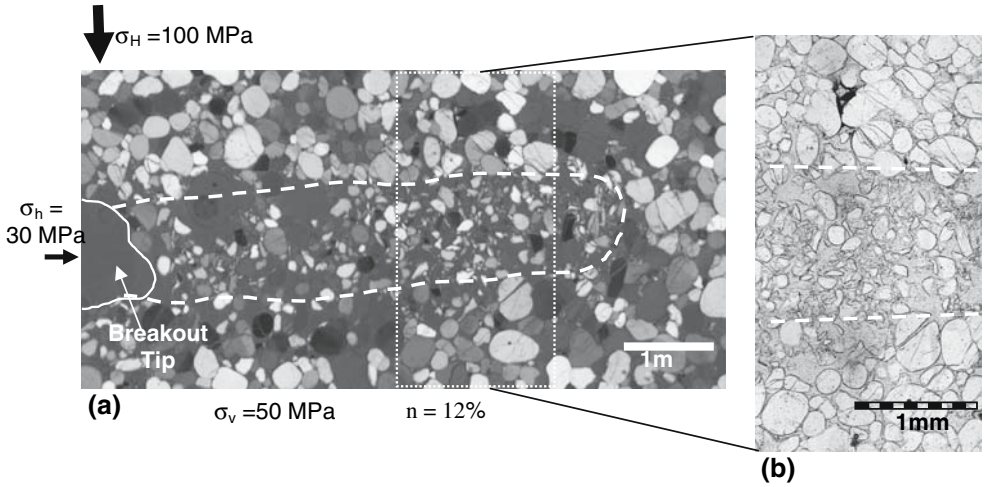

Fig. 4 **a** Polarized light image of the area ahead of a slot-shaped breakout in 11% porosity St. Peter sandstone. A long band, extending perpendicular to the larger compressive stress in the plane of the band, σ_H, with width similar to that of the breakout, and consisting of mainly crushed grains, is contoured by a *dashed line*. Around this zone, grains are predominantly intact, although many are cracked. **b** Plane light image of an enlarged segment of (**a**). The difference in the condition of grains in the compacted and crushed zone and the two adjacent areas is striking [22, 38]

porosity from 11 to 26% that develop slot-shaped breakouts preceded by localized compaction. The common property of these sandstones is their quartz content of over 90%, and grain bonding by primarily sutured contacts.

Another example of in plane propagation of compaction bands has been observed in experiments by Vajdova and Wong [71]. They conducted axisymmetric compression experiments on samples with a circumferential V-notch. One or a few discrete bands are nucleated by the stress concentration at the notch and then propagate across the specimen. After the bands propagate across the entire specimen cross-section, zones of discrete bands, alternating with uncompacted sandstone, form progressively further from the plane of the notch. That is, the zones of inter-layered bands and uncompacted material thicken or propagate along the specimen axis, normal to the maximum compression [71]. Thus, the pattern is similar to that observed by Wong and coworkers in tests on cylindrical samples without a notch rather than the thickening of the bands of compacted material as observed in the Castlegate sandstone. Extending the work on notched specimens, Tembe et al. [69] have applied linear elastic fracture mechanics to their data. The predicted process zone length of 0.3–0.5 times the notch depth agrees with their microstructural observations. Fortin et al. [17] have also used analysis of acoustic emissions to infer rapid (by comparison with the rate of imposed loading) propagation of bands across the width of the experiment. As in the experiments

of Wong, bands along the axis of the specimen are interlayered with zones of less compacted material.

1.3 Effect on fluid flow

Several experiments have demonstrated that compaction bands dramatically reduce the permeability to flow across them. Holcomb and Olsson [28] conducted flow-through experiments in which acoustic emission locations and apparent permeability were determined simultaneously on specimens experiencing compaction localization. Permeability in these experiments fell by several orders of magnitude during band development and growth. Vajdova et al. [70] also measured permeability during formation of thin, discrete compaction bands in Bentheim sandstone. They found sharp decreases in permeability at the onset of compaction band formation and formulated a relation between plastic strain (representative of the number of compaction bands) and permeability.

Fluid flow simulations based on the petrophysical characteristics, geometry and distribution of CBs in the Aztec Sandstone reveal potential impacts at scales relevant to commercial production and injection in aquifers or reservoirs [14, 37, 64, 66, 68]. These include three-fold increases in operating pressure over band-free sandstone, pronounced channeling of flow along the dominant band trend, and the potential for compartmentalization (i.e., stranded reserves). The potential for the occurrence of localized compaction in sandstone aquifers and reservoirs can seriously degrade their flow characteristics is clearly apparent.

1.4 Compaction localization in other materials

Although compaction bands have been recognized only recently in rock, similar phenomena seem to be common in many porous materials. The micromechanisms of deformation are, however, often quite different than those in rocks, i.e., particle rearrangement, disaggregation and fracturing. For example, in open-celled foams, localized compaction is typically triggered by local buckling of a cell wall.

Nesetova and Lajtai [44] describe what appear to be compaction bands in plaster models with several hole shapes cast into them and subjected to boundary stresses; they called these features ‘‘normal shear fractures’’. Poirier et al. [53] report that an interface between deformed and undeformed drinking straws appears (also, see Weaire and Fortes [73] for additional results on arrays of drinking straws) and subsequently propagates through a simple, 2-D packing model. The interface appears at the first peak in the stress-deformation curve and then propagates at nearly constant stress, similar to the stress deformation behavior observed in Castlegate sandstone [28, 46]. Uniaxial stress experiments on a polycarbonate honeycomb [50] showed saw-tooth stress–nominal strain curves in which the local stress drops are correlated with formation of individual compaction layers, similar to the observations of Baud et al. [6] for rock. For closed-cell aluminum foam, Bastawros et al. [5] found irregular discrete bands. In further work on aluminum foam, Issen et al. [31] and Werther et al. [74] found that multiple discrete bands were often observed prior to peak stress, but that these bands were not through-going structures. The peak stress and subsequent stress drop coincided with the formation of a single through-going band of collapsed material. Additionally, the bands were determined to be low angle compacting shear bands (band normals between 10° and 30° from the most compressive stress direction), consisting predominantly of compaction with some shear offset. Predicted band angles determined from the bifurcation approach to localization (see ‘‘Discussion’’ below) were in good agreement with observed band angles. In a steel foam, the initial bands apparently thicken, ultimately compacting the entire specimen; this mode is also associated with a typical stress-nominal strain response showing an initial stress drop, followed by a shelf and eventual hardening [51]. Olsson (personal communication, 2005) has observed the formation and propagation of compaction bands in both a closed-cell polymer foam and a polymer filled with glass microballoons.

1.5 Theoretical frameworks

Different theoretical approaches have been applied to describe the formation or nucleation of compaction bands and their extension. The former has been addressed primarily within the framework of bifurcation theory, similar to that used to describe shear bands [8, 60]. This approach seeks to determine the constitutive response for which a homogeneous state of deformation can give way to an inhomogeneous state consisting of planar regions of high deformation and regions of low deformation. This analysis is useful for identifying the types of material behavior for which the formation of compaction bands is possible but does not specifically address the evolution or extension of the band once formed.

Several related approaches have focused on understanding the conditions that cause a band to extend to the lengths of 10s of meters that are typically observed in the field [4, 9, 41, 67]. In these analyses, it is assumed that a local inhomogeneity initiates the compaction process (possibly because the constitutive properties, as identified by the bifurcation theory, are favorable) and that the band grows due to a stress concentration at its end. In different treatments, the inhomogeneity is idealized as a contractile

ellipsoidal inclusion [62, 67], an anti-crack [16, 41, 67] or a localized volume reduction [33–36].

1.5.1 Bifurcation approach

Olsson [45] was the first to suggest application of the bifurcation approach to predict the onset compaction localization. Issen and Rudnicki [32], incorporating analyses of Ottosen and Runesson [49] and Perrin and Leblonde [52], elaborated upon Olsson's suggestion by adapting the shear band analysis of Rudnicki and Rice [60] to compaction band formation. They showed that compaction bands can occur in materials that exhibit inelastic compaction (volume decrease due to porosity reduction) and have a yield surface with a cap (the shear stress required to cause further inelastic deformation decreases with mean compressive stress). As for shear bands, deviations from normality (i.e., a non-associated flow rule) promote band formation (although whether a non-associated flow rule is appropriate for the cap surface is unclear from experiments or theory). These predictions are roughly in accord with experimental observations in the sense that formation of compaction bands is observed for stress states on the cap surface but not too near the hydrostatic axis. But quantitative discrepancies exist between stress states and values of material parameters at which bands are predicted and observed. At present, it is only possible to say that observations of compaction bands in the field do occur in the types of rock for which the bifurcation analysis predicts that band formation is possible. Parameters describing the evolution of the inelastic behavior are not sufficiently well constrained to make quantitative comparison possible. A principal difficulty is that the predictions of this approach are sensitive to the description of material behavior. There has been considerable recent effort devoted to understanding the effects of various constitutive assumptions on predictions of compaction localization [11, 29, 56–58].

More elaborate constitutive formulations typically allow predictions that agree better with observations but are under-constrained by available data. For example, Grueschow and Rudnicki [18] have studied an elliptical yield surface with semi-axes that evolve differently with measures of inelastic shear and volume strain and Issen [29] and Challa and Issen [10] examined a two-yield surface constitutive framework to represent the two microstructurally observed damage processes [40, 76]. Thus there is a need for a better understanding of the inelastic deformation of porous rocks and of what microstructural processes need to be incorporated in the macroscopic behavior. Although it is certainly possible to develop more elaborate constitutive models, there is a need for numerical calculations to implement them with realistic boundary conditions representative of experiments and for systematic suites of experiments with which to compare them. Because the level of material characterization that can be obtained from field studies is often limited, further experimental studies are essential.

1.5.2 Compaction band extension

Extension of compaction bands has been addressed primarily from a point-of-view similar to fracture mechanics. That is, the material behavior is assumed to be linearly elastic outside a narrow zone of inelastic compaction and extension of the band is driven by the increase in stress at its end. An alternative approach might be that the presence of the band alters the stress state near it in a way that makes the conditions more favorable for band formation, e.g., as predicted by the bifurcation theory. This approach, however, faces the same uncertainties about the evolution of inelastic strain mentioned above in connection with the bifurcation theory and would undoubtedly require direct numerical solution.

Because compaction bands observed in situ are long and thin, Sternlof and Pollard [65] have suggested that they can be modeled as ''anti-cracks,'' as proposed earlier by Fletcher and Pollard [16] as a model for pressure solution surfaces. Anticracks correspond to Mode I, tensile cracks but with the sign reversed. Although this sign reversal formally predicts interpenetration of the crack surfaces, this interpenetration is interpreted physically as the inelastic compaction that occurs in a narrow, but finite thickness zone. The anti-crack model idealizes the stiffness of the material within the band as a constant traction resisting closure. An appropriate value of this stiffness is, however, unclear. Presumably the volumetric stiffness is greater because of the reduced porosity but, as discussed by Sternlof et al. [67], the shear stiffness might be greater or less than that of the surrounding material. More importantly, at the time of formation, cementation of the bands was likely to be much less than currently exists.

A more elaborate model idealizes a compaction band as a narrow inclusion of elastic material with different elastic constants than the surrounding matrix and subjected to an imposed inelastic compactive strain [62, 67]. If the resulting strain of the inclusion is uniform, then the measured width of the band is proportional to the compactive displacement and, hence, can be used as a proxy for it. If the inclusion is ellipsoidal in shape, then the well known result of Eshelby [15] establishes that the strain in the inclusion is indeed uniform (as long as the imposed inelastic strain is also uniform and the inclusion is isolated, i.e., embedded an infinite linear elastic matrix). The measured widths of the bands in the field are roughly elliptical (Fig. 4a, c in Sternlof et al. [67]). Microstructural observations suggest that the magnitude of the inelastic strain (as

reflected by a porosity decrease of about 10% in the band) does not vary strongly with distance along the band (Figs. 6 and 8 in Sternlof et al. [67]). Although there is certainly some scatter and uncertainty in the field measurements, the model of an ellipsoidal inclusion seems consistent with them.

Rudnicki [62] has examined effects of the inclusion properties, aspect ratio and relative magnitudes of imposed inelastic strain and far field stress on the stress state in the inclusion and adjacent to the tip. He finds that these are relatively insensitive to elastic mismatch over a range much larger than plausible for aspect ratios observed for compaction bands in the field, 10^{-3} to 10^{-4}, inelastic compaction corresponding to roughly 10% porosity change, inferred for the bands in field and laboratory, and representative elastic properties for the matrix material in Valley of Fire. The stress states in the inclusion and adjacent to the tip are largely controlled by the ratio of imposed inelastic strain to far field compressive stress divided by shear modulus. Sternlof et al. [67] also calculate the stress state adjacent to the tip of the band for the more elaborate inclusion model. Although the stress state is not unbounded, as predicted for the anti-crack, they show that for the small aspect ratios, and a plausible range of elastic mismatch, it is elevated many fold over the far field stress. Furthermore, the difference between the stress states predicted by the inclusion and anti-crack models decreases sharply with distance away from the band tip. On the basis of these results, the anti-crack model appears to be a reasonable approximation to the more elaborate inclusion model, at least for predicting stresses outside the band.

On the basis of elasticity solutions and computations with a spring network model Katsman et al. [35, 36] have suggested that compaction bands are better represented by ''anti-dislocations''. The distinction appears, however, to be largely one of terminology rather than substance. In both approaches the stress elevation at the band end arises primarily from imposed inelastic compactive strain, or ''localized volume reduction'' as Katsman et al. [36] refer to it. Although Sternlof et al. [67] refer to their model as an ''anti-crack'', they implemented it for compaction bands by using the observed width variation of the band as a proxy for the inelastic compaction and specifying this as the ''crack-surface'' displacement [67]. Because they approximated the measured widths as elliptical, this corresponds to a solution with uniform crack surface traction. On the other hand, Katsman et al. [35] approximate the band shape as tabular.

To the extent that compaction bands can be approximated as an anti-crack, the condition for band extension can be expressed as a critical value of the energy released per unit advance, analogous to the standard practice in fracture mechanics. Using a very simple model of a semi-infinite compaction band in an infinite strip of width h, Rudnicki and Sternlof [61]) derive an expression for the energy released per unit advance as

$$G = \sigma_+ \xi h \varepsilon^p$$

where σ_+ is the uniaxial stress far ahead of the band tip, ξh is the band thickness (with $\xi \ll 1$, corresponding to a thin band), and ε^p is the uniaxial, inelastic compactive strain. This expression pertains if the elastic moduli of the band and surrounding material are not too different but Rudnicki and Sternlof [61] give a correction for this case. Although the model does not necessarily imply a specific band shape or distribution of ε^p, it does assume that the thickness and inelastic strain reach asymptotic values at some large distance behind the tip. Although there is some suggestion that this is the case for the measurements of Sternlof [63], the data are very limited for long, isolated bands. Based on the observations of Sternlof et al. [67], Rudnicki and Sternlof [61] estimate G = 40 kJ/m^2. This value is within the range, 6–43 kJ/m^2 inferred from the stress-strain curves on notched laboratory samples [69, 71] as an upper bound on the compaction energy. The rock types and stress levels are significantly different in the field and laboratory. At present, there are too few measurements to determine whether the similarity is coincidence or reflects common features of band extension in the two settings.

2 Open issues

Currently, there is convincing evidence from both the laboratory and the field that localized zones of compaction can form in porous materials under compressive stress states. A theoretical basis for predicting the possibility of compaction localization using the bifurcation approach is in rough accord with experimental observations. An approach based on nucleation and propagation of an anti-crack has been used as a framework to describe field observations. Yet, neither theory and computation nor experimental and field observations have progressed to the point where reliable predictions can be made about the existence or nature of localized compaction in subsurface reservoirs where it would strongly affect fluid flow. More fundamentally, the factors responsible for the various manifestations of compaction localization observed in the laboratory and the field are not known. Determining these factors is essential if a systematic study is to be made of the physical conditions and material properties associated with compaction band formation. Obviously, there is a need for additional field examples of compaction localization and at the same time for a better understanding of the conditions that give rise to compaction bands in the laboratory.

Specific issues are discussed in more detail in the following sections.

2.1 How frequently do compaction bands occur in the earth?

At present we cannot answer this question. Currently localized compaction has been observed in outcrops in two areas. Because these outcrops occur in the weak porous rocks that are representative of many reservoirs, the observations suggest the possibility that localized compaction is common in the Earth. Furthermore, localized compaction has been observed in laboratory tests under different conditions and in different rocks and is common in a variety of other porous materials. If compaction localization is common to porous formations in the earth, there should be more field examples. If field occurrences of compaction bands are indeed exceptional and such bands are not common in the earth, then the question becomes why not, given the increasing frequency with which they are being observed in rocks in the laboratory and their common occurrence in other porous materials.

One possibility is that such features are indeed ubiquitous, but are not recognized because we are not looking for them. Absent unusual conditions such as differences in susceptibility to erosion or discoloration due to mineral deposition, compaction banding is not easy to observe in the field. Even in well-prepared, clean laboratory specimens compaction localization is difficult to detect from the exterior. Almost certainly compaction localization has been missed in earlier laboratory experiments. The earliest example we have found of experimentally-induced compaction localization in rock was described in the 1994 Masters thesis of Muhuri [42] (cited in Muhuri [43]). Clearly compaction bands were produced during triaxial testing of Berea sandstone, but dismissed at the time in the absence of a framework for their interpretation. Until recently, a similar situation pertained to field studies.

To date, there have also been no reports of compaction localization observed in cores. Again, this is not surprising for several reasons. First, until recently no one knew to look for such a feature. Second, compaction bands are localized features, lacking shear or opening offsets. Thus they will be difficult to detect by surface or borehole geophysical methods, particularly if the compacted zones are as narrow as those in the laboratory and field outcrop examples.

How could compaction bands be detected in situ? The feature being sought is possibly only centimeters in thickness, with lateral extents of perhaps 100s of meters. Very high resolution measurements of density or a related property such as elastic wave velocities should be able to detect the changes induced by compaction localization if they are analogous to what is observed in the laboratory. Similar techniques could also be applied to retrieved core. Overpressuring of fluids trapped between compacted zones might lead to detectable pore pressure jumps. If, however, bands have a vertical orientation, as in the Valley of Fire, then detection in vertical boreholes would be especially problematic.

It is possible that the conditions required for compaction banding rarely occur in the earth. The stresses required are, of course, a function of the material, but Sternlof et al. [67] have inferred that the bands in the Aztec sandstone in the Valley of Fire formed at modest stress levels. The state of stress, not just the magnitude, is also important. Issen and Rudnicki [32] showed that axisymmetric compression is most favorable for compaction localization and recent work by Issen and Challa [30] indicates the intermediate principal stress plays a crucial role in determining whether compaction localization is favored over shear localization. They found that if the stress state was axisymmetric or nearly so, the favored localization mode predicted by a bifurcation theory was compaction in a plane perpendicular to the principal compressive stress. When the intermediate principal stress differed significantly from the minimum, the favored localization mode became shearing. Experimental work to test these theoretical results should be done. In situ, the stress state is unlikely to be truly axisymmetric, but the extent to which the intermediate stress differs from the minimum is difficult to determine as stress determination methods, with the exception of direct overcoring, cannot measure the intermediate principal stress.

2.2 How are laboratory and field compaction bands related?

Certainly, there are similarities between localized compaction observed in laboratory experiments and in the field. Both are roughly planar features with localized reductions in porosity and both form nearly perpendicular to the most compressive stress (although this is often an inference in field studies). Yet there are obvious differences as well. In addition to the vast discrepancy in time and length scales, there are differences in stress magnitude, degree of comminution in the compacted zone, and propagation or thickening modes. In the laboratory, stresses required to induce compaction localization are typically high relative to the stresses inferred for the shallow crust at the time the bands formed in the known field examples. Comminution seems to be a ubiquitous feature of compaction bands in the laboratory, but less so in the field examples. In particular, little comminution was observed in the Valley of Fire bands.

A major difference between band formation as observed to date in the laboratory and in the Earth is that the latter

likely occurred under saturated conditions. These conditions are inferred from the history of the two field sites and, in general, for the shallow crust. Volume changes, such as porosity loss, that occur rapidly by comparison to fluid drainage times induce alterations in pore pressure and, thus, effective stress. The effect of the interaction of altered pore fluid pressure and the evolution of compaction localization and whether it plays a role in the differences between laboratory and field observations is not known. In addition, the role of this interaction is of practical importance since relevant applications invariably involve fluid injection or withdrawal.

2.3 What are the microstructural deformation mechanisms and how do they relate to macroscale behavior and modeling?

Clearly, the processes that occur at the grain-scale, preceding and during compaction localization, determine the macroscale features that we observe and seek to model. Experience has shown that connecting the discontinuous micro scale to the continuous macro scale is difficult. However the increasing sophistication of numerical methods that describe processes at multiple scales may make progress possible. A fundamental objective is to understand the differences in microstructural behavior that cause some materials to exhibit compaction localization and others to not.

Compaction localization has been observed in several sandstones, of varying microstructures, with intact porosities ranging from 11 to 26%. Porosity is not, however, the sole parameter that determines if compaction localization is possible. The recent studies of Haimson and coworkers, discussed earlier, suggest that the degree of quartz suturing at grain contacts is an important factor. Which microstructural attributes enable or promote compaction localization and which inhibit or prevent compaction localization? Answering this question will require systematic field and laboratory investigations together with modeling to determine the localization behavior of sandstones with various microstructures, and to quantify attributes such as grain size, shape, mineralogy, cementation, porosity and the distribution of the attributes (i.e., how homogeneous or heterogeneous is the microstructure) and models of the deformation that occurs at the microscale.

Microstructural differences are likely to play some role in determining, not only if compaction localization occurs, but also the form that it takes. For example, Katsman et al. [34] have suggested a possible explanation for different types of bands based on the results of numerical simulations using a network of spring elements that model different particle sizes and distributions. They found that simulations having a wide range of particle sizes or strengths, produced compaction features that were broad and diffuse. In contrast, those having a narrow range resulted in thin bands.

Understanding the relationship between microstructure and localization behavior requires identification and characterization of the microstructural processes that precede compaction localization, and those that occur as the compaction band forms and propagates. Some examples of porosity-reducing microstructural deformation mechanisms known to be related to compaction localization include grain rotation and rearrangement, grain cracking, grain crushing and pore collapse. Menéndez et al. [40] and Wu et al. [76] report that at least two damage mechanisms appear to be active in some sandstones that exhibit compaction localization: (1) a compactive mechanism, grain crushing and pore collapse; and (2) a dilatant mechanism, axial intragranular cracking and shear-induced debonding. They report uniform cataclastic flow at high confining pressures, due to the first mechanism, and shear localization at low confining pressures, due to the dominance of the second mechanism. Are both these microstructural mechanisms required for compaction localization to occur? More generally, what are the microstructural mechanisms that precede compaction localization, how does microstructural deformation evolve from relatively homogeneous to localized (i.e. what nucleates localization at a particular location), and how do these deformation mechanisms relate to the original microstructural attributes and to the loading path? If different microstructures accomplish compaction localization via different mechanisms, what do these mechanisms have in common?

Although phenomenologically similar forms of compaction localization occur in cellular solids, the microscale deformation mechanisms are completely different. In many cellular solids, porosity reduction is accomplished by cell collapse, typically due to either cell wall buckling or tearing and cracking. In porous rocks, dissagregation, grain rearrangement and fracturing seem to be the primary mechanisms. Are these different manifestations of the same phenomenon, or different phenomena with a superficial resemblance? Can a framework be developed that is capable of representing diverse forms of compaction localization? More generally, are there essential common elements that must be included in, or used to develop, such a framework for describing all forms of compaction localization?

Determining universal micromechanisms or universal characteristics would help to address several questions and needs. A basic one is predicting which materials might exhibit compaction localization or which will not? What controls the number, width and final spatial frequency of the bands? Some materials produce one or two thickening bands, others many discrete thin bands. Is the heterogeneity of representative structural element size an important

determinant of the character of the bands: e.g. are thin bands the result of a narrow range of element sizes and thick, spreading bands associated with a wide range of element sizes?

3 Suggested directions for further research

Ultimately, the importance of research on compaction localization or compaction bands depends on the effects on fluid transport. The large, inhomogeneous strains associated with the formation of compaction bands may also play a role in the structural geology of formations. Little work has been done towards applying the available theoretical, experimental, field and computational results to the interaction between compaction banding and fluid flow in the context of the reservoir rocks that are of such high economic importance. For example, formation of compaction bands as a result of stress changes caused by the injection or withdrawal of fluids or gases would dramatically alter the fluid flow properties of the formation, affecting the efficient, safe and economic uses of the reservoir. A systematic search for more field examples, either in outcrop or core, would be extremely useful.

Additional experimental work is required to fully evaluate existing theoretical frameworks. In particular, development of an adequate constitutive framework requires performance of tests over the full range of mean stress to relate the pre-localization material response (including microstructural deformation processes) to the subsequent localization mode (e.g., localization of compaction or dilation and/or shear). Additionally, predicted localization conditions vary with the value of the intermediate principal stress, relative to the maximum and minimum. Therefore, there is a need to conduct experiments under true triaxial stress states. The experimental work required for understanding the anti-crack mechanism is not as well defined as the identification of inelastic properties needed for the bifurcation mechanism. Further analysis is required to define the material properties and stress states of interest for the anticrack model. The location and cause of the initial compaction process is not clear for the anticrack model. It could be that compaction occurs at the anticrack tip simply due to the high stress concentration there. However, it is also possible that the alteration of stress near the tip of the compaction band makes conditions more favorable for localization conditions. The apparent continued growth of the anticrack by thickening is not well explained nor is the extent to which band propagation is affected by interaction.

Acknowledgment This paper is based on discussions at a workshop sponsored by the U. S. Department of Energy, Office of Science, Geosciences Program. We thank all the participants for written and oral comments that contributed to this article but fully acknowledge that they may disagree with some of the facts, opinions and interpretations expressed here.

References

1. Aydin A (1977) Faulting in Sandstone. Ph.D. dissertation, Stanford University, 246 pp
2. Aydin A (1978) Small faults formed as deformation bands in sandstone. Pure Appl Geophys 116:913–930
3. Aydin A, Johnson AM (1983) Analysis of faulting in porous sandstones. J Struct Geol 5:19–31
4. Aydin A, Borja R, Eichhubl P (2006) Geological and mathematical framework for failure modes in granular rock. J Struct Geol 28:83–93
5. Bastawros A-F, Bart-Smith H, Evans AG (2000) Experimental analysis of deformation mechanisms in a closed-cell aluminum alloy foam. J Mech Phys Solids 48:301–322
6. Baud P, Klein E, Wong T-f (2004) Compaction localization in porous sandstones: spatial evolution of damage and acoustic emission activity. J Struct Geol 26:603–624
7. Beissel S, Belytschko T (1996) On patterns of deformation in phase transformations and Lüders bands. Int J Solids Struct 33:1689–1707
8. Bésuelle P, Rudnicki JW (2004) Localization: shear bands and compaction bands, chapter V, Vol. 89. In: Guéguen Y, Boutéca M (eds) Mechanics of fluid saturated rocks, International Geophysics Series. Academic, London, pp 219–321
9. Borja RI, Aydin A (2004) Mathematical and geologic framework for failure modes in granular rocks. Comput Methods Appl Mech Eng 193:2667–2698
10. Challa V, Issen KA (2004) Conditions for localized compaction of porous granular materials. J Eng Mech 130:1089–1097
11. Challa V, Issen KA (2006) Third invariant dependent single yield surface model and localization conditions for high porosity sandstone. In: Instabilities, bifurcation and degradation in geomechanics, Springer Special Publications (accepted)
12. DiGiovanni AA, Fredrich JT, Holcomb DJ, Olsson WA (2000) Micromechanics of compaction in an analogue reservoir sandstone. In: Girard J, Liebman M, Breeds C, Doe T (eds) Proceedings of the North American Rock Mechanics Symposium, July 31. A.A. Balkema, Rotterdam, pp 1153–1158
13. Du Bernard X, Eichhubl P, Aydin A (2002) Dilation bands, a new form of localized failure in granular media. Geophys Res Lett 29(24):2176, 1029/2002GLO15966
14. Eichhubl P, Taylor WL, Pollard DD, Aydin A (2004) Paleo-fluid flow and deformation in the Aztec Sandstone at the Valley of Fire, Nevada–Evidence for the coupling of hydrogeological, diagenetic and tectonic processes. Geol Soc Am Bull 116(9–10):1120–1136
15. Eshelby JD (1957) The determination of the elastic field of an ellipsoidal inclusion and related problems. Proc Roy Soc Lond A 241:376–396
16. Fletcher RC, Pollard DD (1981) Anticrack model for pressure solution surfaces. Geology 9:419–424
17. Fôrtin J, Stanchits S, Dresen G, Guéguen Y (2006) Acoustic emission and velocities associated with the formation of compaction bands in sandstone, J Geophys Res 111:B10203, doi:10.1029/2005JB003854
18. Grueschow E, Rudnicki JW (2005) Elliptic yield cap modeling for high porosity sandstone. Int J Solids Struct 42:4574–4587
19. Haimson B (2001) Fracture-like borehole breakouts in high-porosity sandstone: are they caused by compaction bands? Phys Chem Earth A 26:15–20

20. Haimson BC (2003) Borehole breakouts in Berea sandstone reveal a new fracture mechanism. Pure Appl Geophys 160:813–831
21. Haimson BC (2006) True triaxial stresses and the brittle fracture of rock. Pure Appl Geophys 163:1101–1130
22. Haimson B, Klaetsch A (2007) Compaction bands and the formation of slot-shaped breakouts in St. Peter sandstone. In: David C (ed) Geomechanics and rock physics for reservoir and repository characterization. Geological Society of London Special Publication (in print)
23. Haimson B, Kovacich J (2003) Borehole instability in high-porosity berea sandstone and factors affecting dimensions and shape of fracture-like breakouts. Eng Geol 69:219–231
24. Haimson B, Lee H (2004) Borehole breakouts and compaction bands in two high-porosity sandstones. Int J Rock Mech Min Sci 41:287–301
25. Haimson BC, Song I (1998a) Borehole breakouts in Berea sandstone: two porosity-dependent distinct shapes and mechanisms of formation, in rock mechanics in petroleum engineering. Soc Pet Eng 1:229–238
26. Haimson BC, Song I (1998b) Mechanics of rock fracturing around boreholes. In: Rossmanith (ed) Mechanics of jointed and faulted rock. A.A. Balkema, Rotterdam, pp 325–330
27. Hill RE (1989) Analysis of deformation bands in the Aztec Sandstone, Valley of Fire State Park, Nevada. M. S. Thesis, Geosciences Department, University of Nevada, Las Vegas, pp 68
28. Holcomb DJ, Olsson WA (2003) Compaction localization and fluid flow. J Geophys Res 108 (B6):2290, doi:10.1029/2001JB000813
29. Issen KA (2002) The influence of constitutive models on localization conditions for porous rock. Eng Fract Mech 69:1891–1906
30. Issen KA, Challa V (2006) Influence of the intermediate principal stress on the strain localization mode in porous rock. J Geophys Res (submitted)
31. Issen KA, Casey TP, Dixon DM, Richards MC, Ingraham JP (2005) Characterization and modeling of localized compaction in aluminum foam. Scripta Mater 52:911–915
32. Issen KA, Rudnicki JW (2000) Conditions for compaction bands in porous rock. J Geophys Res 105(B9):21529–21536
33. Katsman R, Aharonov E (2006) A study of compaction bands originating from cracks, notches and compacted defects. J Struct Geol 28:508–518
34. Katsman R, Aharonov E, Scher H (2005) Numerical simulation of compaction bands in high porosity sedimentary rock. Mech Mater 37:143–162
35. Katsman R, Aharonov E, Scher H (2006a) A numerical study on localized volume reduction in elastic media: some insights on the mechanics of anticracks. J Geophys Res 111:B03204, doi:10.1029/2004JB003607
36. Katsman R, Aharonov E, Scher H (2006b) Localized compaction in rocks: Eshelby's inclusion and the spring network model. Geophys Res Lett 33:L10311, doi:10.1029/2005GL025628
37. Keehm Y, Sternlof K, Mukerji T (2006) Computational estimation of compaction band permeability in sandstone. Geosci J 10(4):499–505
38. Klaetsch AR, Haimson BC (2002) Porosity-dependent fracture-like breakouts in St. Peter sandstone. In: Hammah et al (eds) Mining and tunneling innovation and opportunity. University of Toronto Press, Toronto pp 1365–1372
39. Klein E, Baud P, Reuschle T, Wong T-f (2001) Mechanical behaviour and failure mode of Bentheim sandstone under triaxial compression. Phys Chem Earth (A) 26:21–25
40. Menéndez B, Zhu W, Wong T-F (1996) Micromechanics of brittle faulting and cataclastic flow in Berea sandstone. J Struct Geol 18:1–16
41. Mollema PN, Antonellini MA (1996) Compaction bands: a structural analog for anti-mode I cracks in eolian sandstone. Tectonophysics 267:209–228
42. Muhuri SK (1994) Experimental and microscopic study of the transition form brittle to ductile behavior in the porous Berea sandstone as a function of confining pressure. University of Oklahoma, MS. Thesis
43. Muhuri SK, Scott TE, Stearns DW (2000) Microfracturing in the brittle-ductile transition in Berea sandstone. In: Girard (ed) Pacific rocks 2000, Liebman. Breeds & Doe, Balkema, Rotterdam
44. Nesetova V, Lajtai EZ (1973) Fracture from compressive stress concentrations around elastic flaws. Int J Rock Mech Min Sci Geomech Abstr 10:265–284
45. Olsson WA (1999) Theoretical and experimental investigation of compaction bands in porous rock. Geophys Res Lett 104:7219–7228
46. Olsson W, Holcomb D (2000) Compaction localization in porous rock. Geophys Res Lett 27(21):3537–3540
47. Olsson WA (2001) Quasi-static propagation of compaction fronts in porous rock. Mech Mater 33:659–668
48. Olsson WA, Holcomb DJ, Rudnicki JW (2002) Compaction Localization in porous sandstone: implications for reservoir mechanics, oil and gas science and technology. Revue de l'Institut Français du Pétrole 57(5):591–599
49. Ottosen NS, Runesson K (1991) Properties of discontinuous bifurcation solutions in elasto-plasticity. Int J Solids Struct 27:401–421
50. Papka SD, Kyriakides S (1998) In-plane crushing of a polycarbonate honeycomb. Int J Solids Struct 35(3–4):239–267
51. Park C, Nutt SR (2001) Anisotropy and strain localization in steel foam. Mater Sci Eng A299:68–74
52. Perrin G, Leblond JB (1993) Rudnicki and Rice's analysis of strain localization revisited. J Appl Mech 60:842–846
53. Poirier C, Ammi M, Bideau D, Troadec JP (1992) Experimental study of the geometrical effects in the localization of deformation. Phys Rev Lett 68:216–219
54. Pollard DD, Aydin AA (1988) Progress in understanding jointing over the past century. Geol Soc Am Bull 100:1181–1204
55. Rice JR (1976) The localization of plastic deformation. In: Koiter W (ed) Proceedings of the 14th IUTAM Congress. North Holland, Amsterdam
56. Rudnicki JW (2002) Conditions for compaction and shear bands in a transversely isotropic material. Int J Solids Struct 39:3741–3756
57. Rucnicki JW (2003) Compaction bands in porus rock. In: Labuz JF, Drescher A (ed) Bifurcations and instabilities in geomechanics, Proceedings of the International Workshop on Bifurcation and Instability 2002, St. John's College, Minnesota, June 3–5, 2002. Swets & Zeitlinger (formerly Balkema), pp 29–39
58. Rudnicki JW (2004) Shear and compaction band formation on an elliptic yield cap. J Geophys Res 109:(B03402), doi:10.1029/2003JB002633
59. Rudnicki JW, Olsson WA (1998) Reexamination of fault angles predicted by shear localization theory. Int J Rock Mech Mining Sci 35:512–513
60. Rudnicki JW, Rice JR (1975) Conditions for the localization of deformation in pressure-sensitive dilatant materials. J Mech Phys Solids 23:371–394
61. Rudnicki JW, Sternlof K (2005) Energy release model of compaction band propagation. Geophys Res Lett 32:(L16303), doi:10.1029/2005GL023602, 2005
62. Rudnicki JW (2006) Models for compaction band propagation. In: David C (ed) Geomechanics and rock physics for reservoir and repository characterization. Geological Society of London Special Publication (in print)

63. Sternlof KR (2006) Structural geology, propagation mechanics and hydraulic effects of compaction bands in sandstone. Ph.D. Thesis, Stanford University
64. Sternlof KR, Chapin JR, Pollard DD, Durlofsky LJ (2004) Permeability effects of deformation band arrays in sandstone. AAPG Bull 88:1315–1329
65. Sternlof K, Pollard D (2002) Numerical modeling of compactive deformation bands as granular ''anti-cracks'': EOS Trans. Amer. Geophys. Union, vol. 83 (47), Fall Meeting Supplement, Abstract T11F-10
66. Sternlof KR, Karimi-Fard M, Pollard DD, Durlofsky LJ (2006) Flow effects of compaction bands in sandstone at scales relevant to aquifer and reservoir management. Water Resour Res 42:W07425, doi: 10.1029/2005WR004664
67. Sternlof K, Rudnicki JW, Pollard DD (2005) Anticrack-inclusion model for compaction bands in sandstone. J Geophys Res 110:B11463, doi:10.1029/2005JB0037664
68. Taylor WL, Pollard DD (2000) Estimation of in-situ permeability of deformation bands in porous sandstone, Valley of Fire, Nevada. Water Resour Res 36:2595–2606
69. Tembe S, Vajdova V, Wong T-f, Zhu W (2006) Initiation and propagation of strain localization in circumferentially notched samples of two porous sandstones. J Geophys Res 111:B02409, doi:10.1029/2005JB003611
70. Vajdova V, Baud P, Wong T-f (2004) Permeability evolution during localized deformation in Bentheim sandstone. J Geophys Res 109:B10406, doi:10.1029/2003JB002942
71. Vajdova V, Wong T-f (2003) Incremental propagation of discrete compaction bands: acoustic emission and microstructural observations on circumferentially notched samples of Bentheim sandstone. Geophys Res Lett 30(14):1775, doi:10.1029/2003GL017750
72. Wawersik WR, Rudnicki JW, Dove P, Harris J, Logan JM, Pyrak-Nolte L, Orr Jr FM, Ortoleva PJ, Richter F, Warpinski NR, Wilson JL, Wong T-F (2001) Terrestrial sequestration of CO_2: an assessment of research needs. In: Dmowska R (eds) Advances in geophysics, Vol. 43. Academic, New York, pp 97–177
73. Weaire D, Fortes MA (1994) Stress and strain in solid and liquid foams. Adv Phys 43:685–738
74. Werther DJ, Howard AJ, Ingraham JP, Issen KA (2006) Characterization and modeling of strain localization in aluminum foam using multiple face analysis. Script Mater 54:783–787
75. Wong T-F, Baud P, Klein E (2001) Localized failure modes in a compactant porous rock. Geophys Res Lett 28:2521–2524
76. Wu XY, Baud P, Wong T-f (2000) Micromechanics of compressive failure and spatial evolution of anisotropic damage in Darley Dale sandstone. Int J Rock Mech Mining Sci 37:143–160